Investigation of the nature of light scattering by water

Kovalenko V.F., Levchenko P.G., Shutov S.V. and Bordiuk A.Yu.

Kherson National Technical University, 24 Berislav Highway,
73008 Kherson, Ukraine, E-mail: shutov_sv@mail.ru, zephyrus@ukr.net

Received: 10.08.2008

Abstract

Capabilities of light scattering effects for researches of structural properties of water are analysed. It is shown that measuring of indicatrices of light scattering by water for different incident radiation intensities make it possible to determine degree of water polydispersity, along with dimensions and concentration of scattering centres. We provide information on how the ions contained or gases dissolved in the water, the temperature, structural phase transitions, mechanical influence, purification efficiency and the sources of water affect the characteristics of the scattering centres, thus facilitating some important conclusions about the structure of water clusters.

Keywords: light scattering, water clusters, phase transitions.

PACS: 42.62.-b, 61.20.-p, 61.25.-f, 78.35+c, 78.40.Dw
UDC: 591.044; 577.3

1. Introduction

Light scattering effect is widely used in the studies of parameters of suspended particles in liquids [1, 2]. An interest to investigations of light scattering properties of water is caused by availability of theoretical models involving its cluster structure and possibilities for experimental studies of structural properties of water with the aid of this effect [3].

Now there exist two different points of view regarding the nature of the clusters. One of them consists in representation of the clusters as structurally ordered associates of water molecules having ice-like structure. The existing models of water structure [4] satisfactorily describe the processes of forming of the clusters involving from tens up to hundreds of water molecules, with the size of about 10^{-3} μm and the lifetime about $10^{-10} \div 10^{-9}$ s. Experimental researches have detected a presence in water of long-living formations with the sizes ranging from one tenth of micron up to tens of microns, which are linked with the water clusters [5–7]. However, theoretical models of the clusters with such sizes are still absent. In addition, different research techniques used before are mostly indirect and so they do not allow revealing clear both the nature of these formations and many important details of the water structure – size, shape and concentration of the clusters, their spatial correlation, stability, water scattering degree, etc.

In the works [8, 9] a theory of bubston* clusters has been developed. Bubstons are

* Bubston is an abbreviation of "bubble stabilized by ions".

aggregations of stable gas bubbles which, according to [9], originate in water if even traces of electrolytic dissociation of water molecules are present. Studies of small-angle scattering of laser radiation by the water have detected a presence of micron-sized scattering centres. In opinion of the authors [10], this indirectly confirms a hypothesis of its bubston nature, though no immediate proofs of such an origin of these centres have been presented.

In this work we present results concerning dependences of light scattering by water on the intensity of incident radiation, the content of ions and gases dissolved in it, the water temperature, mechanical action applied to it, as well as the influence of phase transitions "vapour–water" and "ice–water". This has allowed us to extend the capabilities of the method mentioned above and elucidate the nature of the scattering centres in water.

2. Experimental

We measured angular dependence of scattered light intensity $I(\Theta)$ (a so-called scattering indicatrix), where Θ is an angle between the directions of incident radiation and scattered light. A beam of semiconductor laser (a laser pointer with the wavelength $\lambda = 0.65$ μm, the power $P < 1$ mW and the diameter 3 mm) was aimed at a cylindrical glass cuvette under test (the diameter 8 mm), which contained a water. On a holder fixed coaxially with the cuvette, a photodetector (silicon photodiode working in photo-EMF mode, with the photoreception surface diameter of 1.37 mm) was located at the distance of 40 mm away from the cuvette's axis. The photodetector was moved along the arc in the horizontal plane of the laser intensity distribution with the aid of a holder. The geometry of experiment provided the angular resolvability of 2^o. Signal from the photodetector was recorded with a digital multimeter M890C$^+$.

The $I(\Theta)$ dependences were measured in a front half-plane along the direction of incident intensity distribution in the angular range $4^o \le \Theta \le 90^o$, with the step of 2^o. This angular range was chosen since (i) a dominant part of the scattered intensity for the majority of water tests investigated has been concentrated substantially in a small-angle area ($\Theta < 50^o$) and (ii) a part of direct non-scattered beam has not reached the photodetector surface at all under the condition $\Theta \ge 4^o$.

The intensity I_0 of laser radiation was changed using neutral filters. Temperature dependences of the light scattering effect in water were measured in the range of 2^0C÷75^0C. The rest of $I(\Theta)$ measurements were conducted at the room temperature. The content of ions in the water was judged by the value of its resistivity determined with a standard conductometric method.

We investigated light scattering effect for the samples of untreated drinking water and the water additionally purified with a coal filter, distilled water, deionised water and spring water. The selected set of samples allowed tracing influence of purification degree on the light scattering properties in the following series: tap water – water purified with the coal filter – distilled water. The influence of water origin (city water or spring water) was also possible to test.

In order to study the influence of gases dissolved in the water on the light scattering, we used both non-carbonated water and carbonated mineral water of the same origin and various brands.

3. Results and discussion

3.1. Determination of scattering centres size

All the dependences $I(\Theta)$ measured by us represent decreasing functions of the scattering angle, i.e. the directional patterns of the scattered light are forward-stretched. Moreover, the decreasing rates of the $I(\Theta)$ functions decrease with increasing I_0 for the majority of our tests. They also depend on the water origin, being lower for the spring water. In addition, character of $I(\Theta)$ decrease could change from practically smooth (see Fig. 1) to fluctuating (see Fig. 2 and 3). This concerns various water tests of the same origin (see Fig. 1 and 2) and even the same water tests of any origin measured repeatedly after certain time intervals (days, sometimes hours). The above intensity fluctuations differ both in regularity and amplitude. We have observed both single and plural non-periodic fluctuations (see Fig. 2 and 3), as well as periodic ones connected with interference of the scattered light.

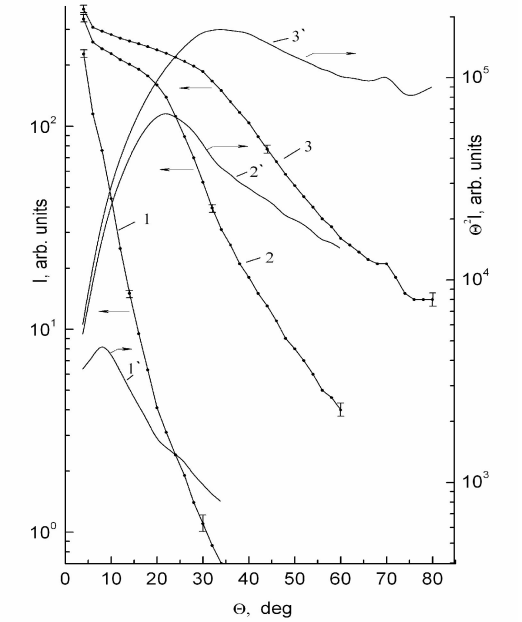

Fig. 1. Scattering indicatrices (curves 1–3) and the corresponding calculated dependences $\Theta^2 I(\Theta) = f(\Theta)$ (curves 1′–3′) for one of the tests of distilled water measured at different incident radiation intensities I_0: 1, 1′ – $0.2I_{0\,max}$, 2, 2′ – $0.6I_{0\,max}$ and 3, 3′ – $I_{0\,max}$.

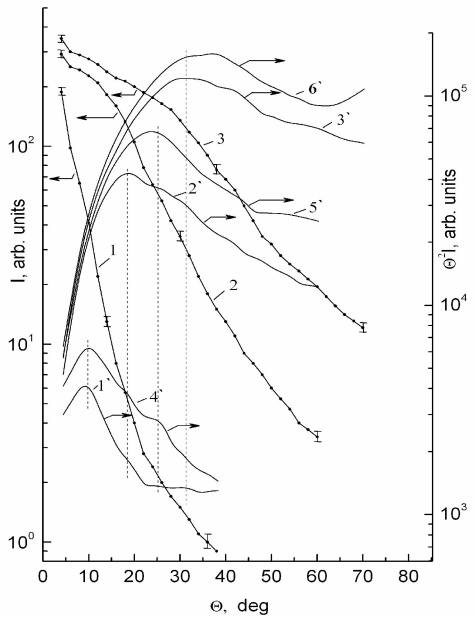

Fig. 2. Scattering indicatrices with I fluctuations (curves 1–3) and the corresponding dependences $\Theta^2 I(\Theta) = f(\Theta)$ (curves 1′–6′) measured at different I_0: 1 – $0.2I_{0\,max}$, 2 – $0.6I_{0\,max}$ and 3 – $I_{0\,max}$. Curves 4′–6′ are calculated on the basis of indicatrices 4–6 (not shown in this figure) obtained two days after the measurements of indicatrices 1–3. Dashed lines show shifts of the basic maximum positions with respect to the subsequent maxima in curves $\Theta^2 I(\Theta) = f(\Theta)$ occurring at increasing I_0.

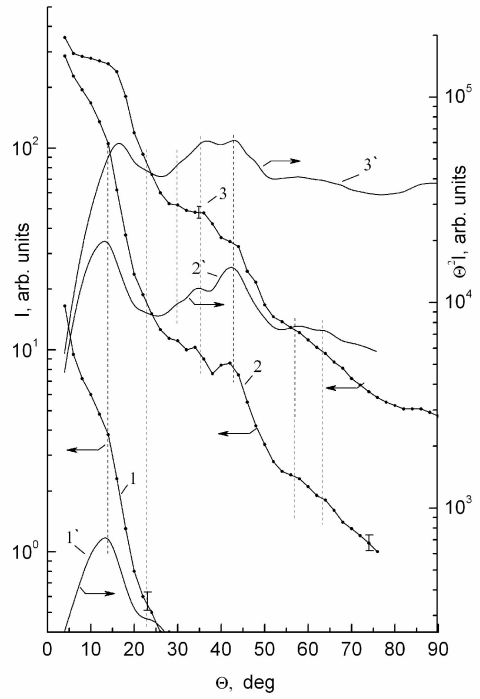

Fig. 3. Scattering indicatrices (curves 1–3) and the corresponding calculated dependences $\Theta^2 I(\Theta) = f(\Theta)$ for one of the tap water tests (no additional purification) measured at different I_0: 1 – $0.2I_{0\ max}$, 2 – $0.6I_{0\ max}$ and 3 – $I_{0\ max}$. Dashed lines show correspondence of the maxima of fine structure of the curves $\Theta^2 I(\Theta) = f(\Theta)$ to the I fluctuations at different I_0.

The scattering indicatrices having periodic fluctuations have not been considered in the present work.

According to [1, 11], frontal oblongness of scattering indicatrices testifies that small-angle scattering is caused by diffraction on centres, of which linear size d is comparable, in the order of magnitude, to the wavelength λ of scattered radiation. Scattering at large angles ($\Theta > 50^o$), typical for the indicatrices measured at the maximum incident intensity and mainly for the spring water, is related to significant contributions of refraction and reflection in the case $d < \lambda$ [1, 11].

In this work a case of light scattering on the system of many particles is realised. However, mathematical apparatus of multiple wave scattering theory is both complex and inconvenient and, moreover, it describes satisfactorily a limited number of cases only. That is why in order to determine the size of the scattering centres, the authors have used Sloan-Arrington technique for the processing of angular dependences of intensity of light scattered by suspended particles, based on theory of light diffraction by spherical or disk-shaped particles. According to the theory mentioned, the angular dependence of the scattered light I_s is described by the equation

$$I_s = J_1^2(X) \big/ kX^2 , \tag{1}$$

where J_1 is the first-order Bessel function, $X = \dfrac{2\pi r}{\lambda`} \sin\Theta`$, $\lambda`$ means the wavelength of the incident light, $\Theta`$ the scattering angle in the medium, $r = 0.5d$ the radius of the scattering particle and k the optical constant given by the expression

$$k = \frac{L^2(\lambda`)^2}{4\pi^2 r^4 I_0} , \tag{2}$$

where L denotes the distance from the photodetector to the axis of cuvette containing liquid under analysis. To determine r after the scattering indicatrix $I(\Theta)$ measured experimentally, Sloan and Arrington [12–14] have simplified the parameter X to the form

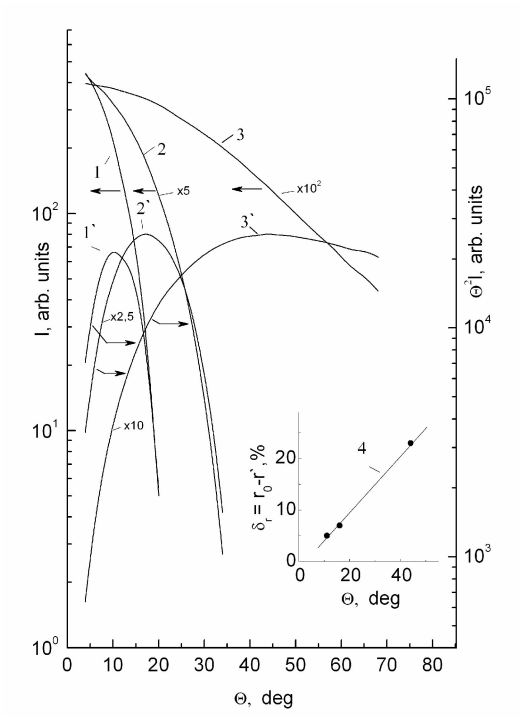

Fig. 4. Scattering indicatrices I_s (curves 1–3) and the corresponding dependences $\Theta^2 I_s(\sin\Theta) = f(\Theta)$ (curves 1′–3′) for different radii r_0 of the scattering centres: 1 – 1.0, 2 – 0.65 and 3 – 0.3 μm. The insert shows dependence of calculated difference between the radius r` found from the maximum positions of 1`–3` curves and a given radius r_0 taken from the scattering angle.

$$X = \frac{2\pi r}{\lambda}\Theta, \qquad (3)$$

where the notations λ and Θ have the same meaning, though being referred to the air. They have suggested to use the following diagram:

$$\lg\left(\Theta^2 I\right) = f\left(\Theta\right), \qquad (4)$$

which transforms initial decrease of the function $I(\Theta)$ into a curve with a maximum. Measurements of scattering indicatrices for the suspensions of both colloid particles and bioparticles with the known sizes determined with electronic or optical microscope have enabled different authors to find out that the angular position of the maximum Θ_{max} of the dependence (4) is given by the relation

$$r\Theta_{max} = 9 - 10 \quad \mu\text{m}\cdot\text{deg}. \qquad (5)$$

Using the Θ_{max} value found graphically, one can determine the radius of scattering particle from Eq. (5). Thus, the diameters of suspended particles in the range $0.2 \le d \le 200$ μm could be found practically independently of their concentration and the refractive index of the medium [12–14]. According to [14], the corresponding error for the diameter does not exceed 10%.

The validity of the Sloan-Arrington technique has also been proved by the fact that the empirical relation (5) agrees with that derived by us on the basis of calculations not involving the approximation $\sin(\Theta)=\Theta$. Fig. 4 shows theoretical indicatrices given by Eq. (1) for different r values and the corresponding dependences given by Eq. (4), where I is replaced by I_s*. The dependence of the difference $\delta r = r_0 - r`$ versus the angle of scattering is also shown in Fig. 4 (see curve 4, where $r`$ are found from the maxima positions of curves 1` to 3` and r_0 are arbitrarily taken values). It is seen that the technique reveals its best accuracy in the small-angle range ($\Theta \le 20°$) where the δr error is < 10%. If we have $\Theta > 20°$, the calculation error for δr increases with increasing Θ. However, it

* Representation in Fig. 1 to 5 of the dependence given by Eq. (4) in the form of relation $(\Theta^2 I) = f(\Theta)$ on semi-logarithmic scale corresponds to the standards [12–18]. It is identical to representation of the dependence $\lg(\Theta^2 I) = f(\Theta)$ on a common linear scale.

has been found in [17] that in this range the error caused by approximations $\frac{\Theta}{\lambda} = \frac{\Theta`}{\lambda`}$ and $\sin\Theta = \Theta$ is compensated by the errors conditioned by refraction and reflection from cuvette's windows. Thus, the method considered provides sufficiently high accuracy in the angular range at least $\Theta \leq 60°$ * [15, 17].

Fig. 1 to 3 show the dependences given by Eq. (4) that correspond to the scattering indicatrices presented in the same figures. Fig. 1 testifies that, in the simplest case of smooth indicatrices, the dependences (1) corresponding to them represent practically smooth functions with a single maximum, which is shifted towards larger scattering angles with increasing I_0. The shape of the curves 1′–3′ (see Fig. 1) is typical for the Sloan-Arrington approximation technique. This allows one to use the latter when determining the size of the scattering centres.

A fine structure of the curves given by Eq. (4) is also available that corresponds to the dependences $I(\Theta)$ under fluctuations of scattered light intensity: a number of additional non-equidistant maxima (see Fig. 2 and 3) manifest themselves near the large-angle dip of the basic (as a rule, the most intensive) maximum. Here the basic maximum in the most cases is shifted to the region of larger scattering angles with increasing I_0, like in the case considered above and, as a rule, it takes place of the additional maximum following it (Fig. 2). The positions of subsequent additional maxima do not depend on the incident radiation intensity I_0. Nonetheless, they become much less resolved with increasing I_0. New additional maxima at larger scattering angles invisible at smaller I_0 (see Fig. 2 and 3) could appear in the dependences given by Eq. (4) while I_0 increases.

A presence of basic maximum on the curves (4) having a fine structure gives ground to expanding the technique for determining the sizes of scattering centres to the cases of non-monotone indicatrices. Displacement of this maximum to the position of that following it, which occurs with increasing I_0, testifies to that the additional maxima are caused by participation of various fixed-sized centres in the light scattering. This enables determining the size of the centres with the technique described above, according to the maxima positions $\Theta_{max(i)}$ (i being the number of the maximum) observed in the curves (4). Here the error of estimation of the r parameter is caused mainly by inaccuracies of Θ_{max} angle, which do not exceed ±6%.

In our opinion, dependence of the scattering indicatrices and the curves (4) upon I_0 is caused by the following features of diffraction on the scattering centres. It is known [19] that the minimum object size d_{min} for which diffraction still takes place may be written as

$$d_{min} \cong \frac{\lambda}{2}. \qquad (6)$$

Connection between d and I_0 could be explained when introducing the «efficiency of diffraction» W, which increases with increasing d value at $d \geq d_{min}$ (i.e., one has the relation $W \sim d$). The integral scattered light intensity I_Σ, i.e. the intensity in the whole range of

* In the work [17] the value $\Theta = 60°$ has been limited merely by the shape of cuvette.

scattering angles, being equal to the area under the curve $I(\Theta)$, is proportional to the «efficiency of diffraction», the concentration N of scattering centres and the incident intensity I_0. Thus, it can be represented as follows:

$$I_\Sigma = \beta WNI_0 \sim \beta dNI_0, \tag{7}$$

where β is a coefficient that takes into account the angular aperture of photodetector, its spectral sensitivity and reversibility of the scattering process.

It is also known [19] that the diffraction divergence of a parallel beam is written as

$$\sin\Theta = \alpha\frac{\lambda}{d}, \tag{8}$$

where α coefficient accounts for diffraction maximum order. It follows from Eq. (8) that decrease in the size of scattering centres produces increase in the angle of diffraction, i.e. a directional diagram for the scattered light becomes less forward-stretched, which would correspond to experimental data occurring under increasing I_0. In this relation it is supposed that the shift of the basic maximum of the curves (4) with increasing I_0 is associated with dominating contribution into the scattered intensity I originated from the particles with smaller d, of which concentration is nonetheless higher than that of larger-scale ones. The contribution into scattering from the small-scale centres at small I_0 is negligible because of a lower «diffraction efficiency».

Simultaneous presence of several maxima in the curves (4) is linked to comparable contributions into the scattering from the centres of various sizes, with the parameters

$$d_1 > d_2 > d_3 > \ldots > d_q, \quad N_1 > N_2 > N_3 > \ldots > dN\,, \tag{9}$$

satisfying the relation

$$d_1N_1I_0 \approx d_2N_2I_0 \approx d_3N_3I_0 \approx \ldots \approx d_qN_qI_0\,, \tag{10}$$

where q is a number of maxima in the dependence (4) for a certain incident intensity I_0. With the condition (9), the increase in I_0 results in displacement towards the right of the series given by Eq. (10). In other words, one is able to reveal more and more small-scale centres of scattering.

If the condition

$$d_1N_1 > d_2N_2, d_3N_3 \ldots d_qN_q\,, \tag{11}$$

holds true and the water is monodispersive, the decreasing rate of the $I(\Theta)$ function (at least in the small-angle region) and the basic maximum position of the dependences (4) do not change with increasing incident intensity (see Fig. 3)[*].

A single maximum on the curves (4) (see Fig. 2) occurs when one of the terms in the series given by Eq. (10) dominates over the others (at a given I_0). Thus, following from Eq. (7), one can judge about the ratio of concentrations N_1 and N_2 of the scattering centres with different sizes d_1 and d_2 on the basis of integral scattered light intensities $I_{\Sigma1}$ and $I_{\Sigma2}$

[*] A negligible shift of the major maximum at I_{0max} in Fig. 3 is obviously caused by nonrigourous fulfillment of condition (11) i.e. $N_1d_1 \geq N_2d_2$.

corresponding to different incident intensities I_{01} and I_{02}. This can be done using the expression

$$\frac{N_1}{N_2} = \frac{d_2 I_{02} I_{\Sigma 1}}{d_1 I_{01} I_{\Sigma 2}}. \qquad (12)$$

In the case of indicatrices with fluctuations, the integral scattering intensity I_Σ represents a total concentration of the centres of various sizes. As seen from Fig. 2 and 3, the greatest contribution to I_Σ at the lowest intensity of incident radiation originates from the scattering on large-scale centres and, to a smaller extent, that on middle-scale ones. For intermediate I_0 values, the major contribution to I_Σ is resulted from the scattering on large and middle-scale centres and, to a lesser degree, scattering on small-scale ones. Finally, if the maximal incident intensity I_0 is used, a portion of the light scattered on small-scale centres increases and I_Σ corresponds fairly well to a total concentration of scattering centres of all sizes.

Table 1 shows the radii r of the scattering particles determined with the technique described above for the water tests of different origins and purification degrees. The changing ranges of the centre sizes observed for different tests of these waters are shown for the tap water with no purification and for additionally purified one. Here the $\bar{I}_\Sigma$ values averaged over several tests for each of the water samples are presented for three I_0 intensities. It is seen from Table 1 that all the water samples under test include a series of large-, middle- and small-scale scattering centres. Further on they are simpler referred to as large, middle and small (the corresponding radii of the centres being $r > 0.9$ μm, $0.4 \le r \le 0.9$ μm and $r < 0.4$ μm, respectively). It is worth noticing that there is good agreement between the size of large centres observed in the angular region $\Theta \le 10^0$ and the value $r = 1.3$ μm given in the study [10]. The latter corresponds to the maximum of size distribution function of scattering particles in the given angular region.

Table 1. Parameters of scattering centres

Origin and preparation of water	r, μm	I_Σ, arb. units		
		0,2 I_0	0,6 I_0	I_0
Unpurified tap water	1.06–1.50; 0.86–0.95; 0.41–0.59; 0.29–0.39	2200	5500	7740
Tap water purified with the coal filter	1.0–1.27; 0.50–0.95; 0.45–0.48; 0.29-0.31	2000	5660	7910
Distilled water	1.12; 0.43; 0.28 1.06; 0.53; 0.40; 0.32; 0.23 1.00; 0.53; 0.40; 0.32; 0.30; 0.27	1750	4500	7110
Spring water	1.06; 0.58; 0.43; 0.34; 0.24; 0.18; 0.17; 0.14	1300	5250	8260

A presence of the centres of 3–4 different sizes is typical for the unpurified tap water, the water purified with the coal filter and, in some cases, the distilled water. For the majority of distilled water tests the centres of 5–6 sizes are revealed. Thus, a decrease in

the concentration of large centres and middle and small centres in the distilled water takes place in the sequence of water samples specified above. On the whole it does not exceed 20%. The spring water is most polydispersive: it could contain the centres of 8–9 various sizes, mostly small ones, of which concentration exceeds that of the similar centres in the tests of other waters. This is confirmed by higher I_Σ values at the largest intensity of incident radiation [*].

Thus, we have proved that the technique suggested by us enables determining the size of scattering centres, their concentration and the water polydispersity degree from the measurements at different incident radiation intensities.

3.2. Studies of the nature of scattering centres

To ascertain reliability of the theory of bubston clusters, we have studied the dependence of I_Σ on the water resistivity ρ, which is inversely proportional to the total content of ions. According to the theory [9], the number of bubston clusters should arise with increasing ion radius and then the integrated intensity of the scattered light should increase, too.

Table 2 shows the values of ρ, I_Σ and r for the water samples of different origins and preparation techniques. As one could see from Table 2, the deionised water has the highest resistivity, integrated intensity of the scattered light and degree of water polydispersity. Its parameters ρ and I_Σ exceed the corresponding parameters for the tap water, which are the lowest, respectively by 250 and 1.6 times. The integrated intensities of light scattering for the rest of samples are close to the I_Σ value for the tap water and do not correlate with the corresponding ρ changes [†].

Table 2. Electrophysical and light scattering parameters of the water samples under test

Origin and preparation of water	I_Σ , arb. units	ρ, kOhm	r, μm
Tap water	14340	4	~1.2; ~0.53; 0.30; 0.24; ~0.19;
Tap water purified with the coal filter	18536	5	~1.2; ~0.42; 0.23; ~0.19
Distilled water	14800	200	~1.06; 0.59; 0.30; 0.24; 0.18; 0.16
Spring water	18150	7	~1.12; 0.48; 0.32; 0.19; 0.16; 0.14
Deionised water	23190	1000	1.19; 0.53; 0.30; 0.23; 0.20; ~0.18; ~0.16; ~0.14

[*] The size of the scattering particles smaller than the diffraction limit (6) has been estimated from the fluctuation peaks on the indicatrices I(Θ) that coincide with the $\Theta_{max\ i}$ positions, as marked by vertical dashed lines in Fig. 2 and 3.

[†] The major contribution to I_Σ for all the samples originates from middle and small scattering centres with $r \leq 0.6$ μm.

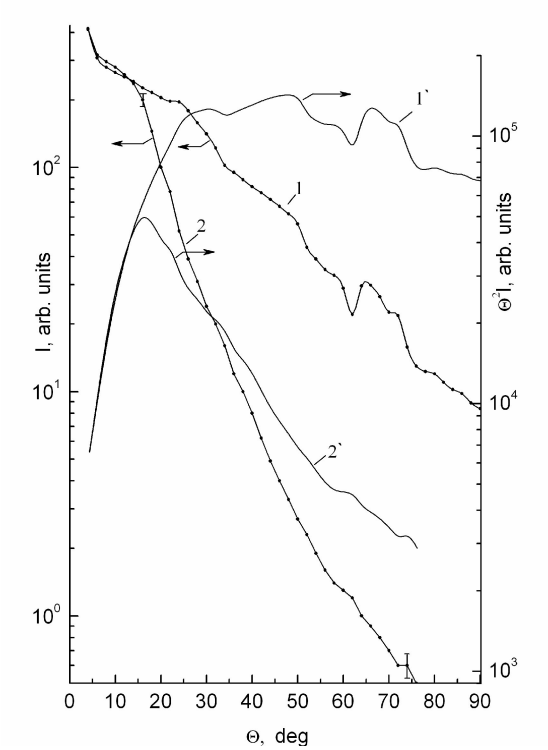

Fig. 5. Scattering indicatrices (curves 1 and 2) measured at I_{0max} and the corresponding calculated dependences $\Theta^2 I = f(\Theta)$ (curves 1` and 2`) for the non-carbonated (1, 1`) and carbonated (2, 2`) mineral waters “Bonaqua”.

The largest I_Σ for deionised water testifies to the highest total concentration of scattering centres, when compare to the other samples studied. The data obtained by us contradict the conceptions of the bubston theory. As specified above, the latter suggests that the water with a minimum content of ions should manifest the lowest concentration of the gas bubbles and, therefore, a minimum I_Σ value. Hence, it follows that, (i) the bubbles of gas, i.e. the bubston clusters, do not represent the scattering centres and, (ii) the ions destroy those centres or prevent their formation. The latter fact is testified by a higher polydispersity of the deionised water.

Fig. 5 illustrates the scattering indicatrices for the "Bonaqua" water (for the both cases of absence of gases and availability of saturated CO_2 gas) and the corresponding calculated dependences (4). Table 3 represents the resistivity, integrated intensity of scattered light and the radii of scattering centres found for these water samples. As seen from Fig. 5 and Table 3, despite of identity of the chemical composition of the samples studied, the presence of dissolved gas in the water leads to the two-fold decrease in I_Σ, smoothing of the corresponding dependence $I(\Theta)$ and reduction of the polydispersity degree for the gas-containing water.

Table 3. Electrophysical and light scattering parameters of the mineral water “Bonaqua”

Samples under test	I_Σ , arb. units	ρ, kOhm	r, μm
Non-carbonated water	24220	6	0.68; 0.40; 0.32; 0.26; 0.20; ~0.16; ~0.14; 0.13
Carbonated water	12600	6	1.19; 0.59; 0.43; 0.30; 0.16

Decrease in I_Σ and smoothing of the scattering indicatrix appearing for the gas-saturated water is due to reduction of concentration and a set of scattering centres. Thus, the molecules or bubbles of the dissolved gas destroy the centres of scattering existing in the non-carbonated water. Efficiency of the destruction increases when the size of the

centres reduces. This is confirmed by a more abrupt slope of the $I(\Theta)$ curve in comparison with the non-carbonated water under increasing scattering angle.

The temperature dependences of the scattering indicatrices are characterised by changes in both the size of the scattering centres and the integrated scattering intensity. The sizes of large ($r > 0.90$ μm) and middle ($0.40 \le r \le 0.90$ μm) centres decrease with increasing temperature and the dependence $r(T)$ for the small ($r < 0.40$ μm) centres has a minimum at $T = 10 \div 20^0$C (see Fig. 6). Here the intensity of scattering by the large centres decreases with increasing temperature, it tends to increase for the middle centres and has a maximum at $T = 10 \div 20^0$C for the small ones.

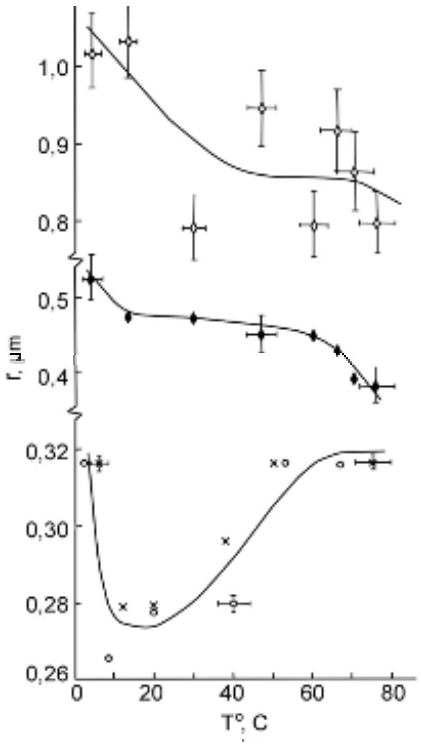

Fig. 6. Temperature dependences of size of the scattering centres for the tap water purified with the coal filter.

Immediately after a phase transition "evaporation–condensation" ($t_e < 10$ min, where t_e denotes the time interval between the end of the transition and the scattering indicatrix measurements, which is hereinafter referred to as the exposition time), the size of the scattering centres is, as a rule, a little bit smaller (about 25%) than that observed for the original water tests. At the same time, the large centres of the original tests could transform to a category of middle ones. With increasing t_e the sizes of the centres change, the character and degree of this change being dependent on the initial sizes of the centres. The dependences $r(t_e)$ for the large and middle centres have a peak at $t_e \approx 2 \div 6$ h, while for the small centres a negligible increase in the size with increasing t_e is typical for the time interval investigated (10 min $\le t_e \le$ 24 h – see Fig. 7).

The integrated intensity of light scattering by the centres of all sizes detected directly after condensation is 15÷40% larger than the I_Σ value for the original tests. With increasing exposition time the scattering intensity gradually decreases and becomes approximately equal to that peculiar for the original samples or somewhat smaller (by about 20%). We are to note that, besides of stable scattering centres which have been observed in the whole t_e interval, unstable centres observable during certain period time are also formed. Some of them are "flickering" – being formed immediately after the condensation, they disappear for a while and then show up again. The periods of appearance and disappearance are from an hour and a half to several hours. A radius of the unstable centres is $r < 0.25$ μm. In some of our experiments a wider set of small stable centres (compared to the original samples of water) has been observed after the condensation.

After a phase transition "freezing–defrosting" the scattering centres of various sizes, including those absent in the initial tests, are being developed. Directly after defrosting the size of the large and middle centres is larger, if compare with the centres available in the original water tests, whereas the r value for the small centres remains practically the same as before freezing (see Fig. 8). The integrated scattering intensity during this period of time is 1.7÷2.0 times less than that for the initial samples. With increasing t_e there occurs a reduction of size of the centres, which is most considerable for the large particles. At the same time, exact character of the dependence $r(t_e)$ for such centres depends upon their initial size. For instance, the process of r decrease for the largest centres is preceded by a period of size stability ($t_e \leq 2$ h – see Fig. 8). Practically invariable scattering intensity corresponds to this period, thus testifying a fixed centre concentration. Consequent decrease in the size of these centres is followed by I_Σ decrease, which is obviously caused by a decrease in their concentration. A size decrease happens immediately after defrosting during $t_e \leq 30$ min for the large centres with $r \leq 1.2$ μm (see Fig. 8). In some cases this results in their total disappearance, while in other cases there occurs stabilization of the r value.

Simultaneously with decrease in the large centre size, small short-living centres absent in the original tests, are being formed (see Fig. 8). As a rule, the sizes of the small

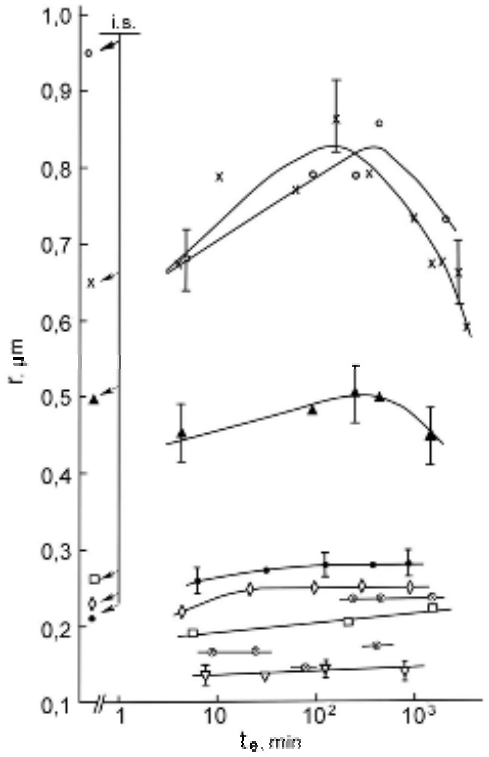

Fig. 7. Time dependences of sizes of the scattering centres for the tap water purified with the coal filter after phase transition "evaporation–condensation" (abbreviation “i. s.” means “initial sizes”).

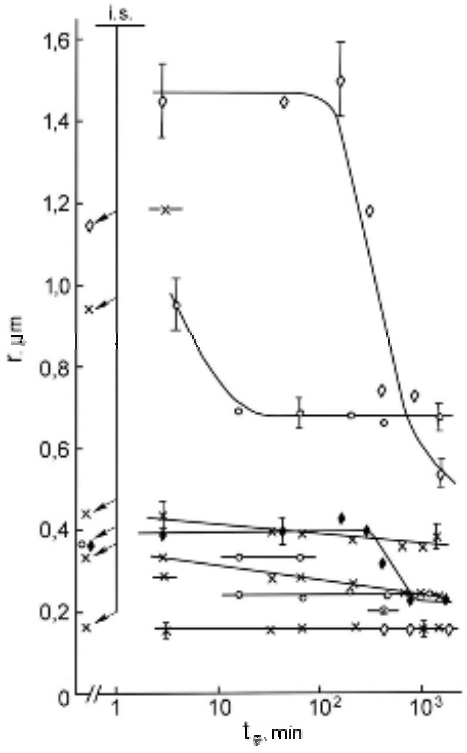

Fig. 8. Time dependences of sizes of the scattering centres for the tap water purified with the coal filter after the phase transition "freezing–defrosting". (abbreviation “i. s.” means “initial sizes”).

stable centres decrease slightly and steadily with increasing t_e. The dependences $r(t_e)$ become weaker with decreasing size of the small centres. At the same time, the sizes of the smallest observable centres do not change in practice over the whole t_e interval. The intensity of light scattering by the small centres increases with increasing t_e and becomes approximately equal to I_Σ for the initial samples in the end of the monitoring period.

Mechanical mixing or shaking of the water, which have been performed within about 2 min, in the most of cases results in increasing size of the scattering centres (5÷20%) or in appearance of new large centres which have not been observed before the mixing. Approximately in 30% of experiments the mixing has resulted in a size decrease appearing for the middle and large centres (10÷15%) or the effect of the mixing has not been seen at all (i.e. the sizes of the centres have remained unchanged). In Table 4 we present the radii of the scattering centres before and after the mixing procedure. The change in the integrated scattering intensity I_Σ occurring after the mixing does not exceed 5% and it does not correlate with the change in the centre sizes.

Table 4. Effect of mechanical mixing on the size of scattering centres

Water sample	*r*, μm (before mixing)	*r*, μm (after mixing)
Distilled water	0.25	0.30
Tap water purified with the coal filter	0.29	0.31
Tap water without additional purification	0.40 0.24	0.68 0.45 0.29
Tap water without additional purification	0.55	0.59
Tap water without additional purification	0.59	0.57
Tap water without additional purification	0.95	1.58 0.95
Tap water without additional purification	1.36	1.58
Tap water without additional purification	1.46	1.22

Characters of influences of all the factors on the size, set and the concentration of the scattering centres certifies that the latter centres cannot be molecules of dissolved impurities, its microparticles or particles of dust. The reasoning is as follows:

1. The sizes of certain molecules are approximately two orders of magnitude less than those of the observable centres and the radiation wavelength. The last circumstance eliminates possibility for diffraction by them.

2. In a would-be case of scattering by some impurity microparticles or particles of dust, a decrease in the integrated scattering intensity should have been expected with increasing purification degree, which has not been observed in our experiments. Moreover, in this case it is practically impossible to explain nontrivial dependences of scattering centre parameters on different factors and parameters changing in the process of water keeping.

The data presented by us evoke the assumption that the centres of scattering are rather microcrystals of ice (clusters) present in the liquid phase of water in the whole temperature range of its natural occurrence. Indeed, a decrease of r and I_Σ with increasing temperature (being typical mainly for the large clusters) would be obviously a consequence of their partial thermal destruction and, as a result, a decrease of their concentration, in agreement with the data known from the work [5]. A certain intensity increase for the scattering by the middle clusters is apparently linked to increase of their concentration, which could occur due to partial destruction of the large centres and their conversion into the middle-scale category.

The reasons for abrupt decrease in the radii of the small centres and subsequent increase occurring with increasing concentration of these centres, accompanied by further reduction under increasing temperature in the range of $2^0\text{C} \le T \le 50^o\text{C}$ (as follows from the dependences $r(T)$ and $I_\Sigma(T)$) are not yet clear. It should be noted that less notable changes and scattering of r and I_Σ parameters for these centres (when compare to the same parameters for the large and middle ones) occurring with increasing temperature confirm their higher thermal stability.

The data concerned with the effect of the phase transitions also indicate a cluster nature of the scattering centres. According to [5], the clusters are being destroyed during evaporation. This statement agrees with reduction of the centre size observed immediately after condensation (see Fig. 3). However, simultaneous appearance in the most of cases of the centres with various sizes just after condensation ($t_e \approx 5 \div 8$ min) in the same set as in the initial tests stipulates the assumption that during the "vapour–water" phase transition the clusters are also preserved in the vapour phase, being destroyed only partially. Otherwise, in the case of total destruction of the initial clusters and formation of new ones it would be difficult to explain their different growth rates and formation of their former set immediately after the condensation.

The fact that the I_Σ parameter after condensation exceeds its initial value indicates increasing concentration of various size centres immediately after the transition. The change in the cluster size and some reduction of their concentration, which are confirmed by decrease in I_Σ occurring with increasing exposition time t_e, are evidently caused by transition of the water from non-equilibrium state to a new equilibrium one, as a result of natural process of structuring characterised basically by decreasing sizes of large and middle clusters.

According to the work [5], monolithic crystal structure of ice disintegrates into the fragments of various sizes during the phase transition "ice-to-water" (see Fig. 8). The changes in the cluster sizes and their concentration during the exposition time and after the transition "vapour-to-water" are obviously attributed to transition of the water from a non-equilibrium state to a new equilibrium one. This state is caused by a natural structuring characterised, as mentioned above, by a size reduction of all stable clusters, along with formation of small unstable centres which could presumably be fragments of the large clusters destroyed during natural structuring. As follows from Fig. 8, in contrast to

the initial water samples, the samples of water measured after holding within a day have not contained the large scattering centres. However, they have had basically fine-scattered cluster structure. Probably, the melting water phenomenon consists precisely in this.

Probably, attachment of the smallest clusters by unsaturated hydrogen bonds occurring owing to reduction of intercluster distance conditions the increase in the cluster sizes during the mixing. In some cases the energy of mixing apparently exceeds the binding energy of hexagonal oxygen rings of the clusters, thus resulting in their partial destruction and reduction of their size.

4. Conclusions

1. The dependence of water scattering characteristics on the intensity of incident radiation revealed by us is associated with the features of diffraction by the particles having sizes close to the diffraction limit. Exploration of this dependence expands information abilities of the scattering technique and, in particular, allows determining the degree of water polydispersity and judging the concentration of the scattering centres included in the water.

2. The bubbles of gas do not represent the scattering centres, i.e. the theory of bubston clusters seems to be inconsistent. Saturation of water with carbon dioxide destroys the centres of scattering existing in the non-carbonated water.

3. The experimental results obtained by us and concerned with the influence of different factors (namely, the temperature, presence of ionised particles and dissolved gas, the time and mechanical factors, phase transitions and origin of the water) on the parameters of scattering centres support the conclusion that the latter centres should be water clusters.

References

1. Van der Hyulst G, Scattering of light by small particles. Moscow: Inostr. Literatura (1961) p. 187.
2. Bezrukova A G and Vladimirskaya I K, 1982. Informational content of light scattering parameters at research of cells. Tsitologiya. **24**: 507–521.
3. Bunkin N F and Lobeyev A V, 1993. Fractal structure of bubstons clusters in water and water solutions of electrolytes. JETP Lett. **58**: 91–97.
4. Sarkisov G N, 2006. Structural models of water. Usp. Fiz. Nauk. **176**: 833–845.
5. Sinitsin N I, Petrosjan V I, Yelkin V A, Devjatkov N D, Guljaev Yu V and Betskij O V, 1999. A special role of the system «millimeter waves - water environment» in the nature. Biomedical Radioelectronics. **1**: 3–21.
6. Zenin S V, Polanuer B M and Tjaglov B V, 1997. Experimental proof of the presence of water fractions. Homeopathic Medicine and Acupuncture. **2**: 37–42.
7. Smirnov A N, Lapshin V B, Balyshev A V, Lebedev I M, Goncharuk V V and Syroeshkin A V, 2005. Water structure: giant heterophase water clusters. Chemistry and Technology of Water. **2**: 11–37.
8. Bunkin N F and Karpov V B, 1990. Optical cavitation of transparent liquids at broadband laser irradiation. JETP Lett. **52**: 669–673.

9. Bunkin F V and Bunkin N F, 1992. Bubstons: stable microscopic gas bubbles in weak electrolytic solutions. JETP. **101**: 512–527.
10. Bunkin N F, Suyazov N V and Tsipenyuk D Yu, 2005. Low-angle scattering of laser radiation by stable micron-scale formations in twice-distilled water. Quantum Electronics. **35**: 180–184.
11. Shifrin K S, Light scattering in turbid medium. Moscow–Leningrad: Gostehteorizdat (1951) p. 288.
12. Arrington C H, Papers presented at the 125th National Meeting of American Chemical Society. Kansas City: Mo (1954).
13. Sloan C K, Papers presented at the 125th National Meeting of American Chemical Society, Kansas City: Mo (1954).
14. Fiel R J, 1970. Low-angle light scattering of bioparticles. I. Model systems. Exp. Cell Res. **59**: 547–551.
15. Fiel R J, Mark E H and Munson B R, 1970. Low-angle light scattering of bioparticles. III. Vaccinia Virus. Arch. Biochem. Biophys. **141**: 547–551.
16. Fiel R J and Scheintaub H M, 1973. Low-angle light scattering of bioparticles. IV. Spleen cells and liver nuclei. Arch. Biochem. Biophys. **158**: 164–170.
17. Livesey P J and Billmeyer Jr F W, 1969. Particle-size determination by low-angle light scattering: new instrumentation and a rapid method of interpreting data. J. Colloid and Interface Sci. **30**: 447–472.
18. Meehan E J and Gyberg A E, 1973. Particle-Size Determination by Low-Angle Light Scattering: Effect of Refractive Index. Appl. Opt. **12**: 551–554.
19. Landsberg G S, Optics (6th edition). Moscow: Fizmatlit (2006) p. 848.

Анотація. *В роботі проаналізовані можливості використання явища розсіяння світла для дослідження структурних властивостей води. Показано, що вимірювання індикатрис розсіяння світла водою, при різних інтенсивностях падаючого випромінювання робить можливим визначити ступінь полідисперсності води та концентрацію і розмір центрів розсіяння. Представлено дані про те, як вміст іонів або газів, розчинених у воді, температура, структурні фазові переходи, механічний вплив, ефективність очистки і джерела походження води впливають на характеристики центрів розсіяння, приводячи до висновків щодо структури водних кластерів.*